

人字齿轮承载接触分析的模型和方法

王 成¹, 方宗德¹, 贾海涛², 张顺利¹

(1. 西北工业大学 机电学院, 陕西 西安 710072; 2. 中国船舶重工集团公司第七〇三研究所, 黑龙江 哈尔滨 150036)

摘 要: 针对人字齿轮啮合特点, 建立人字齿承载接触分析的模型。首先采用有限元方法计算得到工作齿面网格结点的柔度系数, 通过插值获得啮合周期内全部瞬时接触椭圆长轴离散点的柔度系数。根据啮合周期内各接触位置轮齿啮合情况组成齿面接触点法向柔度矩阵, 并通过叠加获得齿轮副的齿面法向柔度矩阵。考虑轴变形对齿面柔度矩阵的影响, 将轴变形产生的附加矩阵叠加到齿面法向柔度矩阵中, 从而获得齿轮系统的柔度矩阵。然后根据轮齿变形位移协调方程, 引入力平衡条件和非嵌入条件, 建立人字齿轮接触问题的数学规划模型, 以一对试验人字齿轮为例, 通过对承载传动误差的比较, 测量幅值与理论幅值分别为 0.451 669'' 和 0.439'', 二者相差很小, 验证了所建模型的正确性。

关 键 词: 人字齿轮; 承载接触; 法向柔度矩阵; 规划

中图分类号: TH132; O242 文献标识码: A

引 言

人字齿轮因具有承载能力高, 工作平稳性好等优点^[1], 在舰船后传动中被大量采用。轮齿承载接触分析(LTCA)是对轮齿承载啮合过程进行数值仿真的一种重要分析方法, 是连接齿轮几何设计与力学分析的桥梁。国内、外许多学者对轮齿承载接触分析做了较深入的研究^[2~6], 但工作主要集中在单斜齿和锥齿轮等方面, 对于人字齿轮而言, 研究较少^[7~8]。本研究基于有限元柔度矩阵的非线性规划法^[9], 针对人字齿轮的啮合特点, 提出了一种将人字齿轮几何分析和力学分析有机地结合在一起的 LTCA 模型及相应的计算方法。

1 齿轮系统的柔度矩阵

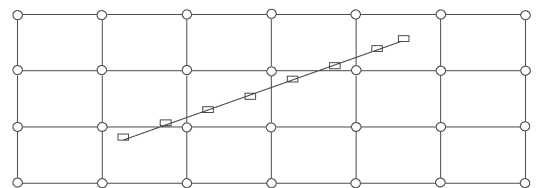
齿轮系统的柔度矩阵包括两部分, 一部分为齿面自身作用单位法向载荷时产生的齿面接触点法向柔度矩阵, 另一部分为因轴的变形而影响其齿面柔度矩阵产生的附加柔度矩阵。

1.1 齿面接触点法向柔度矩阵

1.1.1 齿面接触点柔度系数 λ_{ij}

λ_{ij} 的定义为当齿面 i 点作用一个单位法向载荷时, j 点产生的法向位移。本研究假设载荷只令被作用的轮齿产生位移, 对另一端的轮齿无影响。同时, 为方便起见, 这里仅表述人字齿轮一端斜齿接触点柔度系数的计算, 另一端的计算方法是完全一样的。

将相啮合的一端斜轮齿对进行有限元网格划分。假定该对轮齿的工作齿面有 N 个网格角节点, 利用有限元计算得到 $N \times N$ 个网格节点柔度系数 $\lambda_{ij} (i=1, 2, \dots, N; j=1, 2, \dots, N)$ 。假定齿面接触线(椭圆长轴)上有 n 个离散点, 通过插值得到 $n \times n$ 个接触点柔度系数 $\lambda_{ij} (i=1, 2, \dots, n; j=1, 2, \dots, n)$ 。图 1 为齿面网格过齿轮轴线平面上的旋转投影示意图, 这样, 通过插值可以得到全部离散点的柔度系数。



图中 \circ 表示插值节点(网格角节点), \square 表示插值点(接触点)。

图 1 网格旋转投影示意图

1.1.2 一个啮合周期内齿面接触点法向柔度矩阵

1.1.2.1 瞬时接触椭圆长轴离散点的柔度矩阵

假定瞬时接触椭圆长轴上有 n 个离散点, 则其法向柔度矩阵为:

$$[\lambda] = \begin{bmatrix} \lambda_{11} & \dots & \lambda_{n1} \\ \vdots & \ddots & \vdots \\ \lambda_{1n} & \dots & \lambda_{nn} \end{bmatrix} \quad (1)$$

1.1.2.2 同一啮合位置一端多斜齿对同时啮合时的法向柔度矩阵

对于一端多斜齿对同时啮合的情形,认为齿轮轮齿的承载历程是完全按轮齿重复的。

设有 M 对轮齿同时啮合,并且假设载荷只令被作用的轮齿产生位移,对相邻的轮齿无影响。在当前的接触位置上,每个轮齿的瞬时接触椭圆长轴离散点的法向柔度矩阵分别为 $[\lambda]_1, [\lambda]_2 \dots [\lambda]_M$, 则在这一啮合位置上, M 对轮齿总的法向柔度矩阵为:

$$[\lambda] = \begin{bmatrix} [\lambda]_1 & & & 0 \\ & [\lambda]_2 & & \\ & & \ddots & \\ 0 & & & [\lambda]_M \end{bmatrix} \quad (2)$$

1.1.2.3 同一啮合位置人字齿法向柔度矩阵

假定在某一啮合位置,左端轮齿有 M_1 对轮齿同时啮合,右端轮齿有 M_2 对轮齿同时啮合,并且假设载荷只令被作用的轮齿产生位移,对另一端的轮齿无影响。则在这一啮合位置上,人字齿轮的法向柔度矩阵为:

$$[\lambda] = \begin{bmatrix} [\lambda]_1 & & & & & 0 \\ & \ddots & & & & \\ & & [\lambda]_{M_1} & & & \\ & & & [\lambda]_2 & & \\ & & & & \ddots & \\ 0 & & & & & [\lambda]_{M_2} \end{bmatrix} \quad (3)$$

1.1.2.4 一个啮合周期内人字齿法向柔度矩阵

假定一个周期有 N 个啮合位置,则人字齿轮总的法向柔度矩阵为:

$$[\lambda] = \begin{bmatrix} [\lambda]_1 & & & 0 \\ & [\lambda]_2 & & \\ & & \ddots & \\ 0 & & & [\lambda]_N \end{bmatrix} \quad (4)$$

相啮合齿轮的大、小齿轮的法向柔度矩阵都可以按以上方法计算,将大、小齿轮法向柔度矩阵叠加,即可计算得到齿轮副的齿面离散点的法向柔度矩阵。

1.2 轴变形产生的附加柔度矩阵

齿轮啮合传动时因轴的变形而影响其齿面柔度矩阵。基于有限元分析,将轴离散为若干单元来计算齿轮轮齿受到单位法向力作用时轴节点处的弹性变形(包括弯曲变形和扭转变形)。

挠度 y_{pq} 和扭转角 φ_{pq} 分别为在轴节点 p 相应的齿面结点处施单位法向载荷时,轴节点 q 处产生

的挠度和扭转角。假定将轴分为 N 个节点,利用有限元计算得到 $N \times N$ 个节点挠度 y_{pq} 和扭转角 φ_{pq} ($p=1, 2, \dots, N; q=1, 2, \dots, N$)。这样,可以得到小齿轮轴和大齿轮轴在齿轮轮齿受到单位法向力作用时轴节点处的弹性变形量。

根据文献 [10],可以计算得到由于轴变形而影响其齿面柔度矩阵产生的附加柔量。

同样,通过插值可以得到齿面全部离散点的附加柔度系数(这里需要说明的是,轴的变形不仅令被作用的轮齿产生位移,而且对另一端轮齿也有影响)。与求齿面接触点法向柔度矩阵类似,最终可以获得一个啮合周期内人字齿齿面离散点附加柔度矩阵。

1.3 齿轮系统的柔度矩阵

将轴变形产生的齿面接触点附加矩阵叠加到齿面接触点法向柔度矩阵中从而获得齿轮系统的柔度矩阵。即齿轮系统中柔度矩阵的元素为:

$$f_{pq} = \lambda_{pq} + \delta_{pq} \quad (5)$$

式中: λ_{pq} —齿面接触点法向柔度系数; δ_{pq} —附加柔度系数。

2 齿面接触的数学规划模型^[11]

2.1 位移协调方程

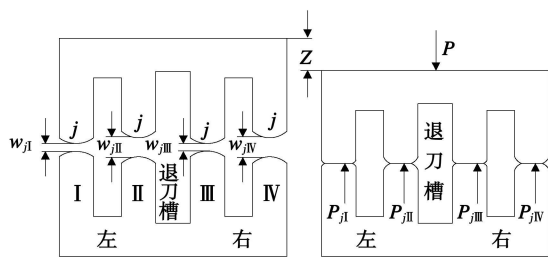


图2 加载接触分析模型

图2为加载接触分析模型。假设在某一啮合位置左右两端各有两对齿(I、II、III和IV)同时接触(某个啮合位置有几对齿同时接触,是通过TCA来给定,然后通过LTCA来确定),图中所示的是齿面过瞬时接触椭圆长轴的法截面。设 j 点为瞬时接触椭圆长轴上的离散点,轮齿变形前,齿对I、II、III和IV的齿面初始间隙为:

$$[w]_k = [\delta]_k + [b]_k, k = I, II, III, IV \quad (6)$$

其中, $[w]_k = [w_1, w_2, \dots, w_n]^T$; $[b]_k = [b_1, b_2, \dots, b_n]^T$; $[\delta]_k = [\delta_1, \delta_2, \dots, \delta_n]^T$ 。

式中: n —瞬时接触椭圆长轴上离散点的个数; b_j ($j=1, 2, \dots, n$)—齿对 k 的齿面法向间隙,具体求解

方法可以参照相关文献[12]; δ -齿对 k 的传动误差(由 TCA 确定)。

在载荷 P 作用下, 轮齿发生弹性变形。设小轮固定, 大轮在载荷作用下沿法向运动 Z 。由于齿面变形, 两齿面由点接触扩展成面接触, 此时忽略瞬时接触椭圆接触区的宽度, 因此认为是沿瞬时接触椭圆长轴发生线接触。

变形后位移协调方程为:

$$[F]_k [p]_k + [w]_k = [Z] + [d]_k \quad (7)$$

其中, $k = I, II, III, IV$; $[p]_k = [p_1, p_2, \dots, p_n]^T$;

$[d]_k = [d_1, d_2, \dots, d_n]^T$; $[Z] = Z[1, 1, \dots, 1]^T$

式中: $p_j (j = 1, 2, \dots, n)$ —齿对 k 的瞬时接触椭圆长轴离散点 j 处的法向载荷; $d_j (j = 1, 2, \dots, n)$ —齿对 k 的瞬时接触椭圆长轴离散点 j 处变形后的齿面间隙; Z —轮齿的法向位移; $[F]_k$ —齿对 k 的法向柔度矩阵。

2.2 力平衡条件

离散载荷 $p_j (j = 1, 2, \dots, n)$ 满足:

$$\sum_{j=1}^n p_{jI} + \sum_{j=1}^n p_{jII} + \sum_{j=1}^n p_{jIII} + \sum_{j=1}^n p_{jIV} = P \quad (8)$$

人字齿轮的特点是左右轮齿所产生的轴向推力可以相互抵消, 即:

$$\sum_{j=1}^n p_{jI} \cos \alpha_{jI} + \sum_{j=1}^n p_{jII} \cos \alpha_{jII} = \sum_{j=1}^n p_{jIII} \cos \alpha_{jIII} + \sum_{j=1}^n p_{jIV} \cos \alpha_{jIV} \quad (9)$$

式中: α —法向载荷与轴向的夹角(取锐角)。

2.3 非嵌入条件

若 $p_{jk} > 0$, 则 $d_{jk} = 0$; 若 $p_{jk} = 0$, 则 $d_{jk} > 0$ 。

2.4 加载轮齿接触分析

采用数学规划法求解加载轮齿接触问题, 则:

$$\begin{cases} \min \sum_{j=1}^{4n+2} X_j \\ -[F][p] + [Z] + [d] + [X] = [w] \\ [e]^T [p] + X_{4n+1} = P \\ [e]^T ([p]_1 \cos[\alpha] - [p]_2 \cos[\beta]) + X_{4n+2} = 0 \\ \text{s.t. } p_j, d_j, Z, X_j \geq 0 \\ p_j = 0 \text{ 或 } d_j = 0 \end{cases} \quad (10)$$

式中: $X_j (j = 1, 2, \dots, 4n + 2)$ 为人工变量; $[X] = [X_1, X_2, \dots, X_{4n}]^T$; $[p]_1, [p]_2$ 分别为左右端离散点载荷; $[\alpha] = [\alpha_1, \alpha_2, \dots, \alpha_{2n}]^T$; $[\beta] = [\beta_1, \beta_2, \dots, \beta_{2n}]^T$ 为离散点载荷与轴向的夹角; $[p]$ 中包含 $[p]_1$ 和 $[p]_2$ 。

求解上述数学规划(一个周期内所有啮合位置, 这里我们将一个周期分成 5 个啮合位置), 就可以得

到该周期内齿面载荷分布和承载传动误差。

由于制造和安装误差的存在, 人字齿轮啮合时两端产生的轴向力可能不平衡因而产生的轴向窜动, 这样可以将力平衡条件公式(9)作为判断条件。当轴向力不平衡时, 沿轴向给定一个微小的窜动量(Δz), 重新计算 TCA 与 LTCA, 直到两端产生的轴向力达到平衡。

3 计算实例与结果

以一对齿轮试验件为例, 在高速齿轮试验台上进行带载试验(大轮上施加扭矩为 2 000 N·m), 试验齿轮参数如表 1 所示。齿轮副的支撑情况如图 3 所示。图 4 是计算得到的齿面载荷分布。图 5 为检测与理论计算得到的承载传动误差。

表 1 人字齿轮的参数

| 齿轮参数 | 主动轮 | 从动轮 |
|----------------|------|--------|
| 齿数 z | 31 | 102 |
| 模数 m_n | | 4.5 |
| 压力角 α_n | | 20° |
| 螺旋角 β | | 28.34° |
| 齿宽 B | 90×2 | 90×2 |
| 旋向 | 右左旋 | 左右旋 |
| 退刀槽宽度 W | | 70 |

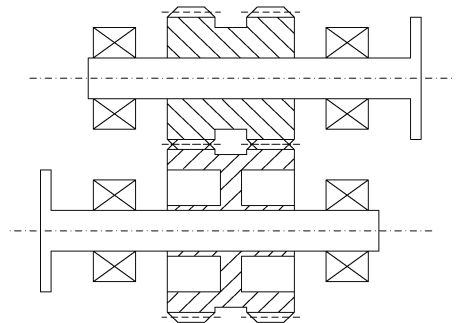


图 3 齿轮传动系统

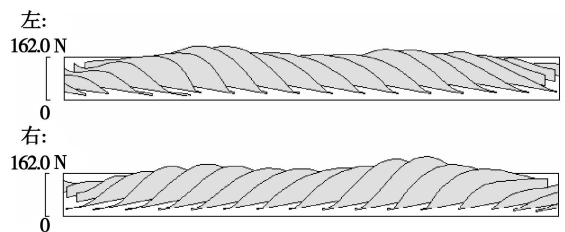
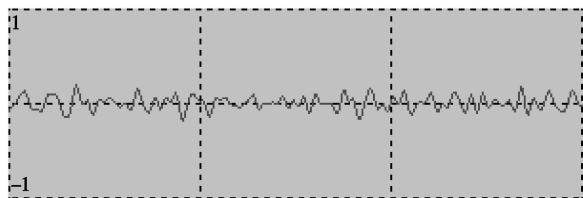


图 4 人字齿轮齿面载荷分布

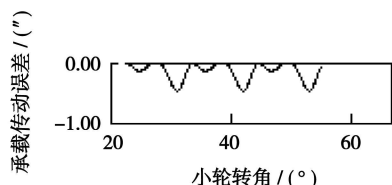
表 2 承载传动误差的检测幅值与理论幅值

| 扭矩 | 承载传动误差幅值/($''$) | |
|-----------|-------------------|-------|
| | 测量幅值 | 理论幅值 |
| 2 000 N·m | 0.451 669 | 0.439 |

从图 5 和表 2 中可以看出: (1) 理论值与检测值能较好的符合; (2) 检测值略大于理论值, 这是因为测量传动误差包括了轮齿变形和齿面微小误差, 而理论传动误差仅包括了轮齿变形。



(a) 测量得到的承载传动误差



(b) 计算得到的承载传动误差

图 5 人字齿轮承载传动误差

4 结 论

(1) 采用有限元方法计算得到工作齿面网格结点的柔度系数, 只需一次有限元计算, 根据啮合周期内各接触位置轮齿啮合情况, 就可以通过插值和叠加获得齿面接触点法向柔度矩阵。

(2) 考虑轴变形对齿面柔度矩阵的影响, 插值得到一个啮合周期内人字齿附加柔度矩阵, 与齿面接触点法向柔度矩阵叠加得到齿轮系统的柔度矩阵。

(3) 根据轮齿变形位移协调方程, 引入力平衡条件和非嵌入条件, 建立人字齿轮接触问题的

数学规划模型。

求解上述数学规划, 将轮齿的承载啮合放在一对齿的模型上进行, 从而可以获得齿面载荷分布和齿轮副的承载传动误差。通过对试验测量得到的承载传动误差与理论计算得到的承载传动误差进行对比(测量幅值与理论幅值仅相差 0.012 669 $''$), 验证了所建模型及求解方法的正确性。

参考文献:

- [1] AMENDOLA B. Single vs double helical gears[J]. Turbomachinery International, 2006, 47(5): 34-38.
- [2] BIBEL G D. Contact stress analysis of spiral bevel gears using finite element analysis[J]. ASME J of Mechanical Design, 1995, 117(2): 235-240.
- [3] GOSSELIN C. Simulation and experimental measurement of the transmission error of real hypoid gears under load[J]. ASME J of Mechanical Design, 2000, 122(1): 109-122.
- [4] 田行斌, 方宗德. 弧齿锥齿轮的有摩擦承载接触分析[J]. 西北工业大学学报, 2000, 18(1): 19-22.
- [5] 周彦伟, 杨宏斌, 邓效忠, 等. 高齿准双曲面齿轮的轮齿加载接触分析[J]. 中国机械工程, 2002, 13(14): 1181-1183.
- [6] 方宗德. 修形斜齿轮的承载接触分析[J]. 航空动力学报, 1997, 12(3): 251-254.
- [7] WINTER, HANS. Load distribution and topological flank modification of helical and double helical gears[J]. European Journal of Mechanical Engineering, 1991, 36(3): 171-176.
- [8] HOCHMANN D, HOUSER D R, THOMAS J. Transmission error and load distribution analysis of spur and double helical gear pairs used in a split path helicopter transmission design//AHS and Royal Aeronautical society. Technical specialists meeting on rotorcraft acoustics/fluid dynamics[C]. Philadelphia; Alexandria, 1991: 15-17.
- [9] 方宗德, 邓效忠, 任东锋. 考虑边缘接触的弧齿锥齿轮承载接触分析[J]. 机械工程学报, 2002, 38(9): 69-72.
- [10] 方宗德, 刘 更, 沈允文. 圆柱齿轮传动的三维接触分析[J]. 西北工业大学学报, 1992, 10(1): 74-78.
- [11] CONRY T F. A mathematical programming technique for the evaluation of load distribution and optimal modifications for gear systems[J]. ASME J of Mechanical Design, 1973, 1115-1121.
- [12] 张金良. 高强度螺旋锥齿轮的设计及实验研究[D]. 西安: 西北工业大学, 2006.

(编辑 伟)

pressure and flash system being compared. The analytic results show that the improved dual-pressure circulation system has a maximum power output and the flash system, however, is simple in structure and flexible in operating modes. Both systems feature relatively wide applications. **Key words:** cement kiln, medium and low temperature waste heat utilization, genetic algorithm, dual-pressure cycle, flash cycle

再燃过程影响因素及燃尽特性研究 = **Study of the Influencing Factors and Burn-out Characteristics of a Re-burning Process**[刊, 汉] / SU Sheng, XIANG Jun, SUN Li-shi, et al (National Key Laboratory on Coal Combustion, Huazhong University of Science and Technology, Wuhan, China, Post Code: 430074) // Journal of Engineering for Thermal Energy & Power. — 2009, 24(4). — 507 ~ 512

With five kinds of coal, including two types of low volatile lean coal, serving as the main fuel, a detailed experimental study was conducted of the reburning process and fuel burn-out characteristics of gaseous fuels on a 36 kW one-dimensional boiler. The test results show that under same conditions, the higher the volatile content of the coal which serves as the main fuel, the greater the denitrification efficiency of the gaseous fuel in the reburning process. When a coal of low volatile content serves as the main fuel, a bigger proportion of gaseous reburning fuel and a long residence time in the reburning zone will be required to attain the same reburning denitrification efficiency as that of a coal with a high volatile content. The test results indicate that even if a low-volatile coal was used as a main fuel, when the gaseous reburning fuel proportion is 10% to 15%, the residence time in the reburning zone reaches 0.7 s to 0.9 s and the excess air factor in the reburning zone is between 0.8 and 0.9, the gaseous fuel reburning process can ensure that the burn-out rate of pulverized-coal particles will not drop significantly. In the meanwhile, under the precondition of the gaseous fuel being sufficiently burned up, a reburning denitrification efficiency of above 50% can be obtained. **Key words:** one-dimension boiler, coal particle, gas fuel, reburning, nitrogen oxide, carbon content of flying ash

600 MW 超临界机组掺烧印尼褐煤、越南无烟煤试验研究 = **Experimental Study of Mixed Combustion of Indonesia-originated Lignite and Vietnam-originated Anthracite in a 600 MW Supercritical Unit**[刊, 汉] / ZHAO Zhen-ning, ZHANG Qing-feng (North China Electric Power Science Research Institute Co. Ltd., Beijing, China, Post Code: 100045), TONG Yi-ying, FANG Zhan-ling (Datang International Power Generation Co. Ltd., Beijing, China, Post Code: 100053) // Journal of Engineering for Thermal Energy & Power. — 2009, 24(4). — 513 ~ 518

An experiment was performed of burning four kinds of bituminous coal, including Shenhua-and-Tashan-originated coal, and Indonesia-originated lignite, in a mixed combustion of Vietnam-originated anthracite on a 600 MW supercritical boiler with its design coal rank being high quality bituminous coal under an opposed-firing mode. Through combustion adjustment, it can guarantee a proportion of 40% Vietnam-originated coal to burn steadily, the coking characteristics of Shenhua and Indonesia-originated coal can be significantly improved. However, the flying ash combustible content increases and the flying ash particle diameter becomes bigger. The test results show that the burn-out of anthracite is more difficult to attain than its ignition and steady combustion. The effective means to solve this problem and give due consideration to the safety of equipment items can be given as follows: the fineness of pulverized coal should be close to the requirement for anthracite combustion to the maximum possible degree while the primary air temperature and its feed rate should be controlled as required for easily-ignited coal ranks. In addition, the concentration of pulverized coal, swirling intensity, centralized oxygen supply, activity of the easily-ignited coal rank and boiler load etc. all exercise a relatively big influence on the combustion of the coal mixture. **Key words:** 600 MW supercritical unit, Indonesia-originated lignite, Vietnam-originated anthracite, mixed combustion

人字齿轮承载接触分析的模型和方法 = **A Model and Method for Load-bearing Contact Analysis of Herringbone Gears**[刊, 汉] / WANG Cheng, FANG Zong-de, ZHANG Shun-li (College of Electromechanical Engineering, North-

west Polytechnic University, Xi'an, China, Post Code: 710072), JIA Hai-tao, (CSIC Harbin No. 703 Research Institute, Harbin, China, Post Code: 150036) // Journal of Engineering for Thermal Energy & Power. — 2009, 24(4). — 519 ~ 522

In the light of the meshing characteristics of herringbone gears, established was a model for load-bearing contact analysis of such gears. First, a finite element method was used to calculate and obtain flexibility coefficients at various grid nodes on the working tooth surface and also the flexibility coefficients through an interpolation at all the long-axis discrete points on the transient contact ellipse during the gear engagement period. On the basis of the gear engagement at various contact locations, a normal flexibility matrix was constituted at the contact points on the tooth surface. Moreover, through a superimposition, a tooth surface normal flexibility matrix of the gear pair was obtained. By taking account of the influence of shaft deformation on the tooth surface flexibility matrix, the additional matrix produced by the shaft deformation was added to the tooth surface normal flexibility matrix to obtain a flexibility matrix of the gear system. Then, based on the gear tooth deformation and displacement coordination equation, the force equilibrium conditions and non-insertion conditions were introduced to establish a mathematical programming model for the contact problem of herringbone gears. Finally, with a pair of herringbone gears under test serving as an example, through a comparison of load-bearing transmission errors (the measured amplitude and theoretical one are 0.451 669 and 0.439 radial second respectively, the difference between the two is very small), the correctness of the established model was verified. **Key words:** herringbone gear, load-bearing contact, normal flexibility matrix, programming

压力对喷动流化床煤气化影响数值模拟 = **Numerical Simulation of the Influence of Pressure on the Coal Gasification in a Spouted Fluidized Bed** [刊, 汉] / DENG Zhong-yi, XIAO Rui, JIN Bao-sheng, SONG Qi-lei (Energy Source Research Institute, Southeast University, Nanjing, China, Post Code: 210096) // Journal of Engineering for Thermal Energy & Power. — 2009, 24(4). — 523 ~ 528

With the aid of a CFD (Computational Fluid Dynamics) software platform, established for the first time was a three-dimensional gasification dynamic model for a spouted fluidized bed. The model included the following sub-models: those for gas-solid flow, coal volatile precipitation and coke gasification reaction, as well as a homogeneous reaction sub-model between gas phases. The model was mainly used to investigate the influence of the change of operating pressure on coal gasification. When the pressure is 0.1 MPa, the mole fractions of carbon monoxide, hydrogen and methane are 8.75%, 10.5% and 3% respectively. When the pressure is 0.3 MPa, the mole fractions of the above items are 11.2%, 12.81% and 4.27% respectively. The quality of coal gas was improved significantly after being pressurized. Finally, the simulation calculated results were verified by test ones. **Key words:** CFD (Computational Fluid Dynamics) model, coal gasification, pressurized spouted fluidized bed, numerical simulation

富钒石煤与生物质在 CFBC 试验台上的混烧实验 = **Mixed Combustion Experiment of Vanadium-enriched Stone Coal and Biomass on a CFBC (Circulating Fluidized Bed Combustion) Test Rig** [刊, 汉] / FAN Xiao-xu (Energy Source Research Institute, Shandong Provincial Academy of Sciences, Jinan, China, Post Code: 250014), NA Yong-jie, LU Qing-gang (Research Institute of Engineering Thermophysics, Chinese Academy of Sciences, Beijing, China, Post Code: 100190), WANG Zhou-ming (Shandong Provincial Development and Investment Co. Ltd., Jinan, China, Post Code: 250014) // Journal of Engineering for Thermal Energy & Power. — 2009, 24(4). — 529 ~ 532

In the light of the specific features of vanadium-enriched stone coal and by utilizing a laboratory-scale CFB (circulating fluidized bed) combustion plant, a mixed combustion experiment was carried out for the stone coal in question and biomass. It was aimed at the comprehensive utilization of resources through vanadium enrichment and heat recovery. The test results show that the stone coal under test is easy to ignite, maintains a steady combustion and displays good burn-out characteristics. This is also the case even when the stone coal is fired with biomass in a mixed combustion. After combustion, the majority of vanadium in the stone coal was transformed to V_2O_5 and became enriched in ash and slag. The stone